



Original article

Coordination of nitro-thiosemicarbazones to ruthenium(II) as a strategy for anti-trypanosomal activity improvement

Claudia Rodrigues^a, Alzir A. Batista^a, Javier Ellena^b, Eduardo E. Castellano^b, Diego Benítez^c, Hugo Cerecetto^c, Mercedes González^c, Letícia R. Teixeira^{d,*}, Heloisa Beraldo^d

^a Departamento de Química, Universidade Federal de São Carlos, 13565-905 São Carlos (SP), Brazil

^b Instituto de Física de São Carlos, Universidade de São Paulo, 13560-970 São Carlos (SP), Brazil

^c Laboratório de Química Orgânica, Facultad de Ciencias–Facultad de Química, Universidad de la República, Iguá 4225, 11400 Montevideo, Uruguay

^d Departamento de Química, Universidade Federal de Minas Gerais, 31270-901 Belo Horizonte (MG), Brazil

ARTICLE INFO

Article history:

Received 7 December 2009

Received in revised form

2 March 2010

Accepted 4 March 2010

Available online 11 March 2010

Keywords:

Thiosemicarbazones

Ruthenium(II) complexes

Anti-trypanosomal activity

ABSTRACT

Complexes [RuCl(H4NO₂Fo4M)(bipy)(dppb)]PF₆ (**1**), [RuCl(H4NO₂Fo4M)(Mebipy)(dppb)]PF₆ (**2**), [RuCl(H4NO₂Fo4M)(phen)(dppb)]PF₆ (**3**), [RuCl(H4NO₂Ac4M)(bipy)(dppb)]PF₆ (**4**), [RuCl(H4NO₂Ac4M)(Mebipy)(dppb)]PF₆ (**5**) and [RuCl(H4NO₂Ac4M)(phen)(dppb)]PF₆ (**6**) with *N*⁴-methyl-4-nitrobenzaldehyde thiosemicarbazone (H4NO₂Fo4M) and *N*⁴-methyl-4-nitroacetophenone thiosemicarbazone (H4NO₂Ac4M) were obtained from [RuCl₂(bipy)(dppb)], [RuCl₂(Mebipy)(dppb)], and [RuCl₂(phen)(dppb)], (dppb = 1,4-bis(diphenylphosphine)butane; bipy = 2,2'-bipyridine; Mebipy = 4,4'-dimethyl-2,2'-bipyridine; phen = 1,10-phenanthroline). In all cases the thiosemicarbazone is attached to the metal center through the sulfur atom.

Complexes (**1–6**), together with the corresponding ligands and the Ru precursors were evaluated for their ability to *in vitro* suppress the growth of *Trypanosoma cruzi*. All complexes were more active than their corresponding ligands and precursors. Complexes (**1–3**) and (**5**) revealed to be the most active among all studied compounds with ID₅₀ = 0.6–0.8 μM.

In all cases the association of the thiosemicarbazone with ruthenium, dppb and bipyridine or phenanthroline in one same complex proved to be an excellent strategy for activity improvement.

© 2010 Elsevier Masson SAS. All rights reserved.

1. Introduction

Trypanosoma cruzi (*T. cruzi*) is the etiologic agent of Chagas disease or American trypanosomiasis [1,2]. Cruzain was shown to be one of the most relevant proteases in *T. cruzi* [2]. Thiosemicarbazones represent an interesting class of compounds with a wide range of pharmacological applications [3] and have been identified as lead scaffolds of cruzain inhibitors [1,2]. Considering that many anti-trypanosomal drugs contain a nitro group, which produces the nitro anion radical, highly toxic to the parasite [4–6], we recently started an investigation of the pharmacological profile of 4-nitroacetophenone-derived thiosemicarbazones. We demonstrated that these thiosemicarbazones and their copper(II) complexes present significant *in vitro* anti-trypanosomal activity, the complexes resulting to be at least 5 times more active than the free ligands. [Cu(4NO₂Ac4M)₂], with *N*⁴-methyl-4-nitroacetophenone thiosemicarbazones (H4NO₂Ac4M) proved to be at

least 12.5 times more active than the thiosemicarbazone counterpart [7].

It has been shown that ruthenium complexes with inhibitors of sterol biosyntheses such as clotrimazole and ketoconazole are more active against *T. cruzi* than the corresponding free ligands [8]. [Ru(Cl₂(CTZ)₂)] (CTZ = clotrimazole) was able to inhibit 90% of the proliferation of epimastigote form of *T. cruzi* at a concentration where the parent compound presented a modest effect. The complex was able to eradicate experimental infection by the highly infective intracellular amastigotes of *T. cruzi* grown on mammalian cells at concentrations as low as 10⁻⁸ mol L⁻¹, which represented a 10-fold enhancement of CTZ's activity [8].

A series of ruthenium(II) complexes derived from 5-nitro-furylsemicarbazones (HL), [Ru^{II}Cl₂(DMSO)₂HL], were developed by some of us, which were able to produce free radicals and redox cycling into the parasite [9]. However, their high protein binding capacity and hydrophilicity did not allow identifying *in vitro* active compounds against *T. cruzi*.

The strategy of linking a nitro-thiosemicarbazone to ruthenium could in principle lead to new anti-trypanosomal drug candidates.

* Corresponding author. Tel.: +55 31 3409 5764; fax: +55 31 3409 5700.

E-mail address: lregina@qui.ufmg.br (L.R. Teixeira).

In the present work ruthenium(II) complexes containing N^4 -methyl-4-nitrobenzaldehyde thiosemicarbazone (H4NO₂Fo4M), or N^4 -methyl-4-nitroacetophenone thiosemicarbazone (H4NO₂Ac4M) and 1,4-*bis*(diphenylphosphine)butane (dppb), 2,2'-bipyridine (bipy), 4,4'-dimethyl-2,2'-bipyridine (Mebipy) or 1,10-phenanthroline (phen) as co-ligands were prepared (Fig. 1).

The nitro-thiosemicarbazones, the new complexes and the ruthenium(II) precursors [RuCl₂(bipy)(dppb)], [RuCl₂(Mebipy)(dppb)], and [RuCl₂(phen)(dppb)], were evaluated for their ability to *in vitro* suppress the growth of *T. cruzi* Tulahuen 2 strain [10].

2. Results and discussion

2.1. Microanalyses and molar conductivity studies

Microanalyses suggest the formation of [RuCl(H4NO₂Fo4M)(bipy)(dppb)]PF₆ (**1**), [RuCl(H4NO₂Fo4M)(Mebipy)(dppb)]PF₆ (**2**), [RuCl(H4NO₂Fo4M)(phen)(dppb)]PF₆ (**3**), [RuCl(H4NO₂Ac4M)(bipy)(dppb)]PF₆ (**4**), [RuCl(H4NO₂Ac4M)(Mebipy)(dppb)]PF₆ (**5**) and [RuCl(H4NO₂Ac4M)(phen)(dppb)]PF₆ (**6**). The molar conductivity data indicate that all complexes are 1:1 electrolytes in accordance with the proposed formulations.

2.2. Infrared spectral studies

In the infrared spectra, the $\nu(\text{C}=\text{N})$ stretching vibrations of H4NO₂Fo4M and H4NO₂Ac4M at 1599 cm⁻¹ and 1590 cm⁻¹ respectively [7,11] remain practically unaltered in the spectra of the complexes, indicating that the imine nitrogen is not involved in coordination. In contrast, the absorption at 830 and 823 cm⁻¹ in the spectra of H4NO₂Fo4M and H4NO₂Ac4M respectively, attributed to the $\nu(\text{C}=\text{S})$ vibration, shifts to 811–815 cm⁻¹ in the spectra of complexes (**1–6**), indicating coordination through the sulfur [12]. Hence, the infrared data suggest coordination of the thiosemicarbazones as monodentate S-donor ligands, as confirmed by the crystal structure determination of complex (**3**) (see Section 2.5).

2.3. ³¹P{¹H} NMR studies

In the ³¹P{¹H} NMR spectra of the complexes two doublets were observed in all cases (see Fig. 2 and Table 1). For complexes (**1–3**) the doublets occur at ca. δ 43 and δ 41 suggesting that one of the phosphorous atoms of dppb is *trans* to the chlorine atom (δ

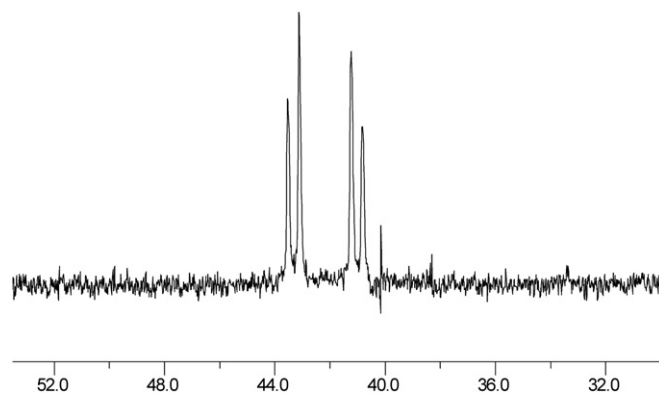


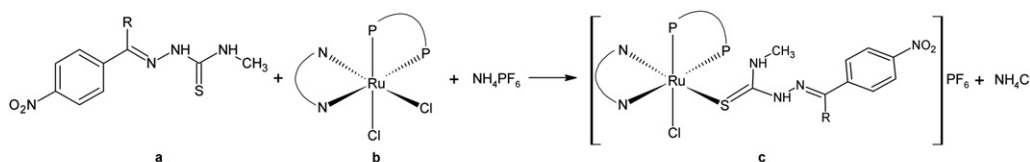
Fig. 2. ³¹P{¹H} NMR spectrum of [RuCl(H4NO₂Fo4M)(bipy)(dppb)]PF₆ (**1**).

43.6–43.3) and the second phosphorous atom is *trans* to the nitrogen of bipyridine, methylbipyridine or phenanthroline (δ 41.6–41.0). For complexes (**4–6**) the doublets were observed at ca. δ 36 and δ 31, indicating again that one of the phosphorous atoms is *trans* to a chlorine (δ 37.5–35.8) and the second phosphorous atom is *trans* to a nitrogen (32.4–30.2) [13]. The difference in the ³¹P{¹H} NMR chemical shifts (ca. 7 ppm) between (**1–3**) and (**4–6**) is probably due to the different electronic effects of H4NO₂Fo4M and H4NO₂Ac4M.

2.4. Electrochemistry

The voltammograms of the thiosemicarbazones show a quasi-reversible process between –0.93 and –1.02 V, which has been attributed to the formation of the Ar-NO₂⁻ radical. The second process between –1.11 and –1.34 V has been assigned to the formation of the Ar-NHOH species, and the irreversible oxidation at 0.17–0.21 V to the formation of Ar-NO. The observed processes correspond to the well known mechanism for nitro-aromatic reduction, as previously proposed by us [7,11] and by other authors [14–17].

The voltammograms of complexes (**1–6**) show a quasi-reversible process ($i_{pa}/i_{pc} \sim 1.1$) attributed to the Ru^{II}/Ru^{III} oxidation (between 0.94 V and 1.09 V) followed by the Ru^{III}/Ru^{II} reduction (between 0.82 and 0.96 V) (see Table 2 and Fig. 3). The high value of



	R	N-N	Yield (%)	
a	H4NO ₂ Fo4M	H	86	
	H4NO ₂ Ac4M	CH ₃	92	
b	[RuCl ₂ (bipy)(dppb)]	-	2,2'-bipyridine	90
	[RuCl ₂ (Mebipy)(dppb)]	-	4,4'-dimethyl-2,2'-bipyridine	81
	[RuCl ₂ (phen)(dppb)]	-	1,10-phenanthroline	77
c	[RuCl(H4NO ₂ Fo4M)(bipy)(dppb)]PF ₆ (1)	H	2,2'-bipyridine	69
	[RuCl(H4NO ₂ Fo4M)(Mebipy)(dppb)]PF ₆ (2)	H	4,4'-dimethyl-2,2'-bipyridine	62
	[RuCl(H4NO ₂ Fo4M)(phen)(dppb)]PF ₆ (3)	H	1,10-phenanthroline	77
	[RuCl(H4NO ₂ Ac4M)(bipy)(dppb)]PF ₆ (4)	CH ₃	2,2'-bipyridine	74
	[RuCl(H4NO ₂ Ac4M)(Mebipy)(dppb)]PF ₆ (5)	CH ₃	4,4'-dimethyl-2,2'-bipyridine	70
	[RuCl(H4NO ₂ Ac4M)(phen)(dppb)]PF ₆ (6)	CH ₃	1,10-phenanthroline	58

P-P = 1,4-*bis*(diphenylphosphine)butane (dppb)

Fig. 1. Synthetic route for complexes (**1**)–(**6**).

Table 1
³¹P{¹H} NMR spectral data for complexes (1–6).

Complex	δ	$^2J_{P-P}$ (Hz)
[RuCl(H4NO ₂ Fo4M)(bipy)(dppb)]PF ₆ (1)	43.3 41.0	33.2
[RuCl(H4NO ₂ Fo4M)(Mebipy)(dppb)]PF ₆ (2)	43.6 41.2	32.4
[RuCl(H4NO ₂ Fo4M)(phen)(dppb)]PF ₆ (3)	43.4 41.6	34.0
[RuCl(H4NO ₂ Ac4M)(bipy)(dppb)]PF ₆ (4)	35.9 30.2	30.9
[RuCl(H4NO ₂ Ac4M)(Mebipy)(dppb)]PF ₆ (5)	35.8 31.8	32.4
[RuCl(H4NO ₂ Ac4M)(phen)(dppb)]PF ₆ (6)	37.5 32.4	34.0

the Ru^{II}/Ru^{III} potential for all complexes indicates electrochemical stability. The formation of the Ar-NO₂⁻ radical has been observed separately in the voltammograms of complexes (3) and (6) but not in those of complexes (1), (2), (4) and (5), indicating that in the latter, once formed the radical reacts immediately. For complexes (1–6) the process occurring between –1.04 and –1.17 V has been attributed to the formation of Ar-NHOH. For all complexes the remaining processes have been assigned to the thiosemicarbazone moiety, as previously proposed by us [18].

Experiments carried out on the main drugs used in Chagas disease treatment, nifurtimox (Nfx, 3-methyl-4-[(5-nitrofurfurylidene)amino]thiomorpholine-1,1-dioxide), a nitrofur derivative, and benznidazole (2-nitro-*N*-(phenylmethyl)-1*H*-imidazole-1-acetamide), a nitroimidazole derivative, suggest that intracellular nitro-moiety reduction followed by redox cycling yielding reactive oxygen species may be their major mode of action against *T. cruzi* [9].

In the present work the quasi-reversible process between –0.93 and –1.02 V has been attributed to the formation of the Ar-NO₂⁻ radical. The reported value for the same process in Nfx [9] falls into this same range. Interestingly, complexes (1–6) have adequate NO₂-reduction potential to act against *T. cruzi* via a redox cycling process. Coordination to ruthenium(II), like in the case of copper(II) [7], affects positively the value of the ligand NO₂-reduction potential (compare E_{pc} of H4NO₂Ac4M, –1.02 V [7], to E_{pc} of complex (6), –0.91 V, Table 2), generating compounds which are more easily reduced in biological media.

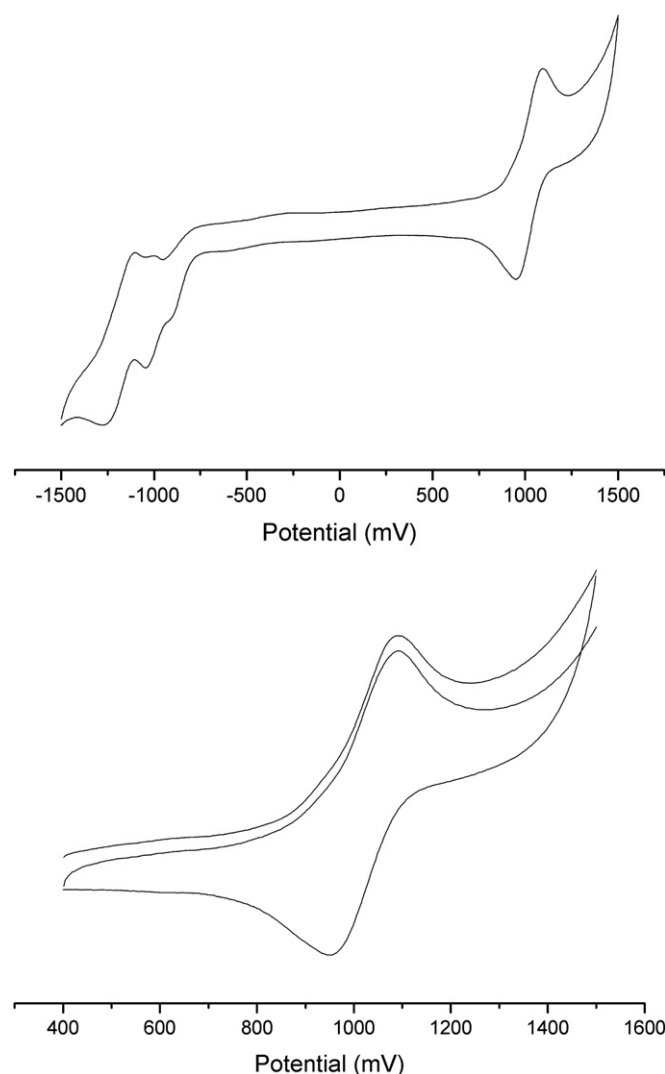
2.5. Crystal structure of complex (3)

Crystal data and refinement results for complex (3) are shown in Table 3. The ORTEP3 view [19] of the structure can be seen in Fig. 4. Table 4 shows selected bond distances [Å] and angles [°].

3 crystallizes in the monoclinic system, P2₁/*n* space group with *Z* = 4. In 3 the thiosemicarbazone in the *EE* configuration is attached to the metal center through the sulfur atom. As expected, all bond distances are very similar in H4NO₂Fo4M and in complex (3).

Table 2
Cyclic voltammetry data (V) for complexes (1–6) (0.100 V s⁻¹, CH₂Cl₂, 0.1 mol L⁻¹, TBAP).

Complex	Ru ^{II} /Ru ^{III}	Ru ^{II} /Ru ^{III}	Ar-NO ₂ ⁻	Ar-NHOH
[RuCl(H4NO ₂ Fo4M)(bipy)(dppb)]PF ₆ (1)	0.98	0.83	–	–1.05
[RuCl(H4NO ₂ Fo4M)(Mebipy)(dppb)]PF ₆ (2)	0.94	0.82	–	–1.16
[RuCl(H4NO ₂ Fo4M)(phen)(dppb)]PF ₆ (3)	1.09	0.96	–0.90	–1.04
[RuCl(H4NO ₂ Ac4M)(bipy)(dppb)]PF ₆ (4)	1.02	0.93	–	–1.17
[RuCl(H4NO ₂ Ac4M)(Mebipy)(dppb)]PF ₆ (5)	1.02	0.87	–	–1.13
[RuCl(H4NO ₂ Ac4M)(phen)(dppb)]PF ₆ (6)	1.06	0.90	–0.91	–1.11

**Fig. 3.** Cyclic voltammogram of [RuCl(H4NO₂Fo4M)(phen)(dppb)]PF₆ (3) (CH₂Cl₂, 0.1 mol L⁻¹ TBAP). Inset: peaks of the ruthenium redox process.

However some bond angles undergo significant variations upon coordination. The C7–N2–N3 bond angle is 116.70(3)° in H4NO₂Fo4M and 113.7(3)° in complex (3). In addition the N3–C8–S and N4–C8–S angles are 118.05(14)° and 124.82(14)° in H4NO₂Fo4M and 121.1(3)° and 121.2(3)° respectively, in complex (3).

2.6. In vitro anti-*T. cruzi* activity

Table 5 shows the effect of all evaluated compounds on the growth of the epimastigote form of *T. cruzi* (Tulahuen 2 strain), expressed as ID₅₀. The ligands proved to be less active than both the reference drug, Nfx, and the ruthenium precursors. H4NO₂Fo4M was more active than H4NO₂Ac4M. The ruthenium(II) complexes (1–6) were more active than their corresponding ligands, nifurtimox (Nfx), and the synthetic ruthenium(II) precursors.

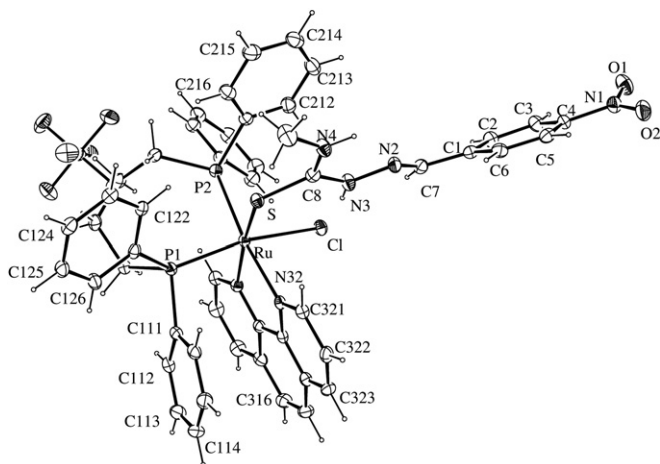
All complexes (1–6) were at least 10 times more active than their corresponding ligands. Complexes (1–3) and (5) revealed to be the most active among all studied compounds. Complexes (1–3) and (5) were 20 times more active than the free thiosemicarbazones. The greatest amount of dose reduction upon coordination to ruthenium was observed for complex (5).

Table 3
Crystal data for H4NO₂Fo4M and [RuCl(H4NO₂Fo4M)(phen)(dppb)]PF₆ (**3**).

Compound	H4NO ₂ Fo4M	[RuCl(H4NO ₂ Fo4M)(phen)(dppb)]PF ₆ (3)
Empirical formula	C ₉ H ₁₂ N ₄ O ₃ S	C ₅₁ H ₅₀ N ₆ O ₂ F ₆ P ₃ SCl ₅ Ru
Formula weight	256.29	1296.26
Temperature, K	293(2)	150(2)
Crystal system	Triclinic	Monoclinic
Space group	<i>P</i> – 1	<i>P</i> 2 ₁ / <i>n</i>
<i>Unit cell dimensions</i>		
<i>a</i> , Å	7.8686(16)	12.0023(3)
<i>b</i> , Å	11.236(2)	26.0686(6)
<i>c</i> , Å	13.795(3)	17.6136(3)
α , °	83.37(3)	
β , °	81.90(3)	100.093(2)
γ , °	85.10(3)	
Volume, Å ³	1196.4(4)	5425.7(2)
Z, Density calc., mg/m ³	4, 1.423	4, 1.587
Absorption coefficient, mm ⁻¹	0.274	0.73
<i>F</i> (000)	536	2632
Crystal size, mm ³	0.199 × 0.543 × 0.231	0.14 × 0.1 × 0.04
θ range for data coll., °	3.09–25.00	3.08–26.06
Index ranges	–8 ≤ <i>h</i> ≤ 9, –13 ≤ <i>k</i> ≤ 13, –16 ≤ <i>l</i> ≤ 16	–14 ≤ <i>h</i> ≤ 14, –32 ≤ <i>k</i> ≤ 32, –17 ≤ <i>l</i> ≤ 19
Reflections collected	28 253	34 021
Independent reflections	4188 [<i>R</i> _{int}] = 0.0367	10 092 [<i>R</i> _{int}] = 0.0652
Completeness	99.5% (to $\theta = 25.00^\circ$)	94.8% (to $\theta = 25.00^\circ$)
Absorption correction	None	None
Refinement method	Full-matrix least-squares on <i>F</i> ²	Full-matrix least-squares on <i>F</i> ²
Data/restraints/parameters	4188/0/341	10 092/0/686
Goodness-of-fit on <i>F</i> ²	1.031	1.038
Final <i>R</i> indices [<i>I</i> > 2σ(<i>I</i>)]	<i>R</i> ₁ = 0.0365, <i>R</i> ₂ = 0.0875	<i>R</i> ₁ = 0.0442, <i>R</i> ₂ = 0.1063
<i>R</i> indices (all data)	<i>R</i> ₁ = 0.0516, <i>R</i> ₂ = 0.0945	<i>R</i> ₁ = 0.0728, <i>R</i> ₂ = 0.1203
Largest diff. peak and hole, e Å ⁻³	0.199 and –0.167	0.734 and –0.882

All ruthenium precursors revealed to be active, [RuCl₂(Mebipy)(dppb)] being the most effective. Interestingly the greatest amount of activity improvement upon association of the precursor with a nitro-thiosemicarbazone was verified for complex (**1**), which is 20 times more active than its ruthenium precursor. The anti-trypanosomal activity of the studied ruthenium precursors was demonstrated for the first time in the present work.

In all cases association of the thiosemicarbazone with ruthenium, dppb and bipyridine or phenanthroline in one same complex resulted to be an excellent strategy for activity improvement.

**Fig. 4.** Perspective view of the structure of [RuCl(H4NO₂Fo4M)(phen)(dppb)]PF₆ (**3**).**Table 4**
Selected bond lengths (Å) and angles (°) for H4NO₂Fo4M and [RuCl(H4NO₂Fo4M)(phen)(dppb)]PF₆ (**3**) (standard deviations in parentheses).

Bond lengths (Å)	H4NO ₂ Fo4M	(3)	Angle (°)	H4NO ₂ Fo4M	(3)
C(8)–S(1)	1.7000(18)	1.703(4)	N(3)–C(8)–S(1)	118.05(14)	121.1(3)
C(8)–N(4)	1.323(2)	1.328(4)	N(4)–C(8)–S(1)	124.82(14)	121.2(3)
C(8)–N(3)	1.354(2)	1.343(4)	C(7)–N(2)–N(3)	116.70(16)	113.7(3)
N(2)–N(3)	1.374(2)	1.381(4)	C(8)–N(3)–N(2)	119.55(16)	120.5(3)
C(1)–C(7)	1.466(2)	1.453(5)	N(2)–C(7)–C(1)	120.77(16)	120.8(3)
N(1)–O(1)	1.228(2)	1.227(4)	O(2)–N(1)–O(1)	122.79(18)	123.9(3)
N(1)–O(2)	1.223(2)	1.223(4)			

Table 5
In vitro anti-*T. cruzi* activities for ligands, ruthenium complexes and synthetic precursors.

	ID ₅₀ (μM) ^{a,b,c}
[RuCl ₂ (bipy)(dppb)]	13.7
[RuCl ₂ (Mebipy)(dppb)]	6.9
[RuCl ₂ (phen)(dppb)]	8.1
H4NO ₂ Fo4M	14.2
[RuCl(H4NO ₂ Fo4M)(bipy)(dppb)]PF ₆ (1)	0.7
[RuCl(H4NO ₂ Fo4M)(Mebipy)(dppb)]PF ₆ (2)	0.6
[RuCl(H4NO ₂ Fo4M)(phen)(dppb)]PF ₆ (3)	0.7
H4NO ₂ Ac4M	>25.0 (31%, [7])
[RuCl(H4NO ₂ Ac4M)(bipy)(dppb)]PF ₆ (4)	2.3
[RuCl(H4NO ₂ Ac4M)(Mebipy)(dppb)]PF ₆ (5)	0.8
[RuCl(H4NO ₂ Ac4M)(phen)(dppb)]PF ₆ (6)	1.2
Nfx	7.7

^a ID₅₀: dose that inhibits 50% of *T. cruzi* growth.

^b The results are the mean values of three different experiments with an SD less than 10% in all cases.

^c Values in parenthesis are PGI (percentage of growth inhibition) at 25 μM.

Comparison of the activities of the previously developed copper (II) complex, [Cu(4NO₂Ac4M)₂] (ID₅₀ = 2.0 μM) [7], with those of the presently studied ruthenium(II) complexes (**4–6**) with the same ligand (ID₅₀ = 2.3, 0.8, and 1.2 μM) reveals that coordination to ruthenium is a better strategy of dose reduction.

2.7. Haemolytic assay

Red blood cell lysis is a simple method widely used to study the damage caused by a compound to a human cell. It provides a quantitative measure of haemoglobin release. In the present work haemolysis was controlled spectrophotometrically 24 h after

Table 6
In vitro haemolytic activities for ligands, ruthenium complexes and synthetic precursors.

	Doses (μM)	Haemolysis percentage (%)
[RuCl ₂ (Mebipy)(dppb)]	50.0 ^a	21.6
H4NO ₂ Fo4M	200.0 ^b	42.3
	50.0	9.0
[RuCl(H4NO ₂ Fo4M)(Mebipy)(dppb)]PF ₆ (2)	50.0 ^a	11.1
H4NO ₂ Ac4M	200.0	2.6
	100.0	0.0
	50.0	0.0
[RuCl(H4NO ₂ Ac4M)(Mebipy)(dppb)]PF ₆ (5)	50.0 ^a	100.0
Positive control (water)	–	100.0
Amphotericin B	1.5	34.4
Nfx	50.0	0.0

^a Solubility problems, in the assayed milieu, were observed at higher concentrations than 50.0 μM.

^b Some solubility problems, in the assayed milieu, were observed at this concentration.

treatment with the studied compounds. We performed the assay for selected compounds (see Table 6). The assayed compounds, except ruthenium complex **5**, displayed lower lysis at 50.0 μM doses than the red blood damaging agent amphotericin B at 1.5 μM . Solubility problems did not allow us to determine the exact ID_{50} values; however the approximate ID_{50} values for ligands, ruthenium complexes and synthetic precursors were similar to or higher to that of Nfx.

3. Conclusions

The developed ruthenium complexes (**1–6**) present a monodentate thiosemicarbazone, which is rarely found in the literature. The foregoing results indicate that the studied compounds might be investigated *in vivo* as anti-trypanosomal agents, since they are able to *in vitro* inhibit the growth of the parasite. Especially complex **2**, with the lowest ID_{50} against *T. cruzi*, resulted non-toxic in the red blood cells assay, presenting a selectivity index (SI), defined as $\text{SI} = \text{ID}_{50, \text{red blood cells}} / \text{ID}_{50, T. cruzi} > 83$. Its SI was higher than the estimated SI values for the corresponding ligand (SI \sim 14) and the ruthenium synthetic precursor (SI $>$ 7) (Table 6). Complex **5** resulted to be more toxic in this assay.

Complexes **1–6** are capable to form the Ar-NO_2^- radical in a potential range similar to that of nitro-containing anti-trypanosomal drugs. Therefore intracellular nitro-moiety reduction followed by redox cycling yielding reactive oxygen species may be one of their modes of action against *T. cruzi*. However, since the ruthenium precursors also present anti-trypanosomal activity other modes of action could take place as well.

It has been suggested for ruthenium complexes with azoles that Ru–DNA binding provides a means of damaging the parasite, and that rapid metal–DNA binding might be a key feature of their therapeutic action [20]. In addition, it has been suggested that in order for DNA binding to take place, a chloro ligand must be replaced by water [21,22].

Hence we may hypothesize that a similar mechanism of Ru–DNA binding could take place in the present case. Moreover, a synergistic effect involving both the nitro-containing ligand and ruthenium was observed, which favored the activity improvement upon coordination. Considering that the thiosemicarbazone binds to the metal center as a monodentate ligand, its release is facilitated, which probably allows both metal and ligand to be easily directed to their biological targets.

4. Experimental

4.1. Physical measurements

Elemental analyses were performed on a Fison equipment, model EA 1108. A Radiometer Copenhagen Meter Lab., model CDM 230 was employed for molar conductivity measurements. Infrared spectra (KBr pellets) were obtained using a BOMEM MICHELSON instrument, model 102. NMR spectra were obtained at room temperature with a Bruker DRX-400 Avance (400 MHz) spectrometer. For $^{31}\text{P}\{^1\text{H}\}$ NMR (161 MHz) measurements CH_2Cl_2 was used as solvent and H_3PO_4 85% as external reference.

The electrochemical experiments were carried out at room temperature in CH_2Cl_2 containing 0.1 mol L^{-1} tetrabutylammoniumperchlorate (TBAP, Fluka Purum) using an electrochemical analyzer from Bioanalytical Systems Inc. (BAS), model 100BW. The working and auxiliary electrodes were stationary Pt foils, and the reference electrode was Ag/AgCl, a medium in which ferrocene is oxidized at 0.48 V (Fc^+/Fc). The voltammogram was performed at a scan rate of 0.100 V s^{-1} , at 298 K.

4.2. X-ray crystallography

Room temperature X-ray diffraction data collection (ϕ scans and ω scans with κ offsets) of $[\text{RuCl}(\text{H}_4\text{NO}_2\text{Fo4M})(\text{phen})(\text{dppb})]\text{PF}_6$ was performed on an Enraf-Nonius Kappa-CCD diffractometer (95 mm CCD camera on κ -goniostat) using graphite-monochromated $\text{MoK}\alpha$ radiation (0.71073 Å). Data were collected up to 50° in 2θ , with a redundancy of 4. The final unit cell parameters were based on all reflections. Data collections were carried out using the COLLECT program [23]; integration and scaling of the reflections were performed with the HKL Denzo–Scalepack system of programs [24]. Analytical absorption correction was applied [25].

The structure was solved by direct methods with SHELXS-97 [26a]. The model was refined by full-matrix least-squares on F^2 with SHELXL-97 [26b]. All hydrogen atoms were stereochemically positioned and refined with the riding model [26b]. Hydrogen atoms of the CH groups were set isotropic with a thermal parameter 20% greater than the equivalent isotropic displacement parameter of the atom to which each one was bonded. This percentage was set to 50% for the hydrogen atoms of the CH_3 group. The programs SHELXL-97 [26b], and ORTEP3 [19] were used within WinGX[27].

4.3. Syntheses of $[\text{RuCl}_2(\text{bipy})(\text{dppb})]$, $[\text{RuCl}_2(\text{Mebipy})(\text{dppb})]$ and $[\text{RuCl}_2(\text{phen})(\text{dppb})]$

$[\text{RuCl}_2(\text{bipy})(\text{dppb})]$, $[\text{RuCl}_2(\text{Mebipy})(\text{dppb})]$ and $[\text{RuCl}_2(\text{phen})(\text{dppb})]$ were prepared according to previously described procedures [28].

4.4. Synthesis of N^4 -methyl-4-nitrobenzaldehyde thiosemicarbazone ($\text{H}_4\text{NO}_2\text{Fo4M}$) and N^4 -methyl-4-nitroacetophenone thiosemicarbazone ($\text{H}_4\text{NO}_2\text{Ac4M}$)

The thiosemicarbazones were prepared as described by some of us [7,11]. Briefly, equimolar amounts of 4-nitrobenzaldehyde and 4-nitrobenzophenone (6.6×10^{-3} mol) were mixed with N^4 -methyl thiosemicarbazide in absolute ethanol (40 mL) with addition of 2–4 drops of concentrated sulfuric acid as catalyst. The reaction mixture was kept under reflux for 6–7 h. The solids which precipitated were filtered and washed with diethyl ether and dried.

4.5. Syntheses of the complexes

The complexes were obtained by dissolving the desired thiosemicarbazone (0.079 mmol) in CH_2Cl_2 (20 mL) with gentle heating and stirring under argon atmosphere. After cooling the solution to room temperature $[\text{RuCl}_2(\text{bipy})(\text{dppb})]$, $[\text{RuCl}_2(\text{Mebipy})(\text{dppb})]$ or $[\text{RuCl}_2(\text{phen})(\text{dppb})]$ (0.079 mmol) and NH_4PF_6 (0.079 mmol) were added. The reaction was stirred at room temperature for 24 h. The solids which precipitated were filtered and washed with diethyl ether and dried *in vacuo*.

4.5.1. $[\text{RuCl}(\text{H}_4\text{NO}_2\text{Fo4M})(\text{bipy})(\text{dppb})]\text{PF}_6$ (**1**)

Red solid. Anal. Calc. ($\text{C}_{47}\text{H}_{46}\text{ClF}_6\text{RuN}_6\text{O}_2\text{P}_3\text{S}$): C, 51.21; H, 4.21; N, 7.62; S, 2.91%. Found: C, 51.47; H, 4.21; N, 7.66; S, 2.95%. IR (KBr, cm^{-1}): ν_{assNO_2} 1540, ν_{sNO_2} 1332, $\nu(\text{C}=\text{N})$ 1589, $\nu(\text{C}=\text{S})$ 815. Molar conductivity (1×10^{-3} mol L^{-1} CH_3COCH_3): 84.4 $\mu\text{S cm}^{-1}$ $^{31}\text{P}\{^1\text{H}\}$ NMR (CH_2Cl_2 δ/ppm): 43.3 (d, $^2J_{\text{P-P}}/\text{Hz}$ 33.2); 41.0 (d, $^2J_{\text{P-P}}/\text{Hz}$ 32.2).

4.5.2. $[\text{RuCl}(\text{H}_4\text{NO}_2\text{Fo4M})(\text{Mebipy})(\text{dppb})]\text{PF}_6$ (**2**)

Red solid. Anal. Calc. ($\text{C}_{49}\text{H}_{50}\text{ClF}_6\text{RuN}_6\text{O}_2\text{P}_3\text{S}$): C, 52.06; H, 4.46; N, 7.43; S, 2.84%. Found: C, 52.52; H, 4.50; N, 7.47; S, 2.85%. IR (KBr, cm^{-1}): ν_{assNO_2} 1538, ν_{sNO_2} 1331, $\nu(\text{C}=\text{N})$ 1597, $\nu(\text{C}=\text{S})$ 814. Molar conductivity (1×10^{-3} mol L^{-1} CH_2Cl_2): 40.6 $\mu\text{S cm}^{-1}$ $^{31}\text{P}\{^1\text{H}\}$ NMR (CH_2Cl_2 δ/ppm): 43.6 (d, $^2J_{\text{P-P}}/\text{Hz}$ 32.4); 41.2 (d, $^2J_{\text{P-P}}/\text{Hz}$ 32.4).

4.5.3. [RuCl(H4NO2Fo4M)(phen)(dppb)]PF₆ (3)

Red solid. Anal. Calc. (C₄₉H₄₈ClF₆RuN₆O₂P₃S): C, 52.15; H, 4.29; N, 7.45; S, 2.84%. Found: C, 52.46; H, 4.31; N, 7.48; S, 2.86%. IR (KBr, cm⁻¹): ν_{ass}NO₂ 1543, ν_sNO₂ 1344, ν(C=N) 1597, ν(C=S) 814. Molar conductivity (1 × 10⁻³ mol L⁻¹ CH₂Cl₂): 40.1 μS cm⁻¹ 31P{¹H} NMR (CH₂Cl₂ δ/ppm): 43.4 (d, ²J_{P-P}/Hz 34.0); 41.6 (d, ²J_{P-P}/Hz 34.0).

4.5.4. [RuCl(H4NO2Ac4M)(bipy)(dppb)]PF₆ (4)

Orange solid. Anal. Calc. (C₄₈H₄₈ClF₆RuN₆O₂P₃S): C, 51.64; H, 4.33; N, 7.53; S, 2.87%. Found: C, 51.90; H, 4.35; N, 7.58; S, 2.90%. IR (KBr, cm⁻¹): ν_{ass}NO₂ 1523, ν_sNO₂ 1338, ν(C=N) 1603, ν(C=S) 811. Molar conductivity (1 × 10⁻³ mol L⁻¹ CH₃COCH₃): 100.6 μS cm⁻¹ 31P{¹H} NMR (CH₂Cl₂ δ/ppm): 35.9 (d, ²J_{P-P}/Hz 30.8); 30.2 (d, ²J_{P-P}/Hz 30.9).

4.5.5. [RuCl(H4NO2Ac4M)(Mebipy)(dppb)]PF₆ (5)

Orange solid. Anal. Calc. (C₅₀H₅₂ClF₆RuN₆O₂P₃S): C, 52.47; H, 4.58; N, 7.34; S, 2.80%. Found: C, 52.68; H, 4.59; N, 7.37; S, 2.82%. IR (KBr, cm⁻¹): ν_{ass}NO₂ 1520, ν_sNO₂ 1344, ν(C=N) 1608, ν(C=S) 813. Molar conductivity (1 × 10⁻³ mol L⁻¹ CH₂Cl₂): 48.9 μS cm⁻¹ 31P{¹H} NMR (CH₂Cl₂ δ/ppm): 35.8 (d, ²J_{P-P}/Hz 32.4); 31.8 (d, ²J_{P-P}/Hz 32.4).

4.5.6. [RuCl(H4NO2Ac4M)(phen)(dppb)]PF₆ (6)

Orange solid. Anal. Calc. (C₅₀H₅₀ClF₆RuN₆O₂P₃S): C, 52.56; H, 4.41; N, 7.36; S, 2.81%. Found: C, 52.76; H, 4.43; N, 7.41; S, 2.84%. IR (KBr, cm⁻¹): ν_{ass}NO₂ 1519, ν_sNO₂ 1342, ν(C=N) 1610, ν(C=S) 812. Molar conductivity (1 × 10⁻³ mol L⁻¹ CH₂Cl₂): 48.8 μS cm⁻¹ 31P{¹H} NMR (CH₂Cl₂ δ/ppm): 37.5 (d, ²J_{P-P}/Hz 34.0); 32.4 (d, ²J_{P-P}/Hz 34.0).

4.6. In vitro anti-trypansomal activity

T. cruzi epimastigotes (Tulahuen 2 strain) were grown at 28 °C in an axenic medium (BHI-Tryptose) as previously described [7,9,10], complemented with 5% fetal calf serum. Cells were harvested in the late log phase, re-suspended in fresh medium, counted in Neubauer's chamber and placed in 24-well plates (2 × 10⁶/mL). Cell growth was measured as the absorbance of the culture at 590 nm, which was proved to be proportional to the number of cells present. Before inoculation, the media were supplemented with the indicated amount of the studied compound from a stock solution in DMSO. The final concentration of DMSO in the culture media never exceeded 1% and the control was run in the presence of 1% DMSO and in the absence of any compound. No effect on epimastigotes growth was observed by the presence of up to 1% DMSO in the culture media. Nifurtimox (Nfx) was used as the reference trypanocidal drugs. The ruthenium precursors were included in these assays to provide information on the trypanocidal effect of these complexes. The percentage of growth inhibition was calculated as follows $\{1 - [(A_p - A_0p)/(A_c - A_0c)]\} \times 100$, where A_p = A₅₉₀ of the culture containing the studied compound at day 5; A_{0p} = A₅₉₀ of the culture containing the studied compound right after addition of the inocula (day 0); A_c = A₅₉₀ of the culture in the absence of any compound (control) at day 5; A_{0c} = A₅₉₀ in the absence of the compound at day 0. To determine ID₅₀ values, parasite growth was followed in the absence (control) and presence of increasing concentrations of the corresponding compound. The ID₅₀ values were determined as the drug concentrations required to reduce by half the absorbance of that of the control (without compound).

4.7. Red blood cell lysis assay [29,30]

Human blood collected in sodium citrate solution (3.8%) was centrifuged at 200 g for 10 min at 4 °C. The plasma supernatant was removed and the erythrocytes were suspended in ice cold PBS. The cells were again centrifuged at 200 g for 10 min at 4 °C. This procedure was repeated two more times to ensure the removal of

any released haemoglobin. Once the supernatant was removed after the last wash, the cells were suspended in PBS to get a 2% w/v red blood cell solution. 400 μL of the studied compounds in PBS (50, 100 and 200 μM), negative control (solution of PBS), or amphotericin B (1.5 μM) were added to 400 μL of the 2% w/v red blood cell solution in ten microcentrifuge tubes for each concentration and incubated for 24 h at 37 °C. Complete haemolysis was attained using neat water yielding the 100% control value (positive control). After incubation, the tubes were centrifuged and the supernatants were transferred to new tubes. The release of haemoglobin was determined by spectrophotometric analysis of the supernatant at 405 nm using EL 301 MICROWELL STRIP READER. Results were expressed as percentage of the total amount of haemoglobin released by action of the compounds. This percentage is calculated using the equation Haemolysis percentage (%) = [(A₁ - A₀)/A_{1 water}] × 100, where A₁ is the absorbance at 405 nm of the test sample at t = 24 h, A₀ is the absorbance at 405 nm of the test sample at t = 0 h, and A_{1 water} is the absorbance at 405 nm of the positive control (water) at t = 24 h. The experiments were performed in quintuplicate.

Supplementary material available

CCDC 702060 contains the supplementary crystallographic data for this paper. These data can be obtained free of charge from The Cambridge Crystallographic Data Centre via www.ccdc.cam.ac.uk/data_request/cif.

Acknowledgments

Financial support from FAPEMIG, CNPq Instituto do Milênio-Inovação e Desenvolvimento de Novos Fármacos e Medicamentos (IM-INOVAR, Proc. CNPq 420015/05-1), CNPq-PROSUL and Fapesp from Brazil, RIDIMEDCHAG-CYTED is acknowledged.

References

- [1] D.C. Greenbaum, Z. Mackey, E. Hansell, P. Doyle, J. Gut, C.R. Caffrey, J. Lehrman, P.J. Rosenthal, J.H. McKerrow, K. Chibale, J. Med. Chem. 47 (2004) 3212–3219.
- [2] S.P. Fricker, R.M. Mosi, B.R. Cameron, I. Baird, Y. Zhu, V. Anastassov, J. Cox, P. S. Doyle, E. Hansell, G. Lau, J. Langille, M. Olsen, L. Qin, R. Skerlj, R.S.Y. Wong, Z. Santucci, J.H. McKerrow, J. Inorg. Biochem. 102 (2008) 1839–1845.
- [3] H. Beraldo, D. Gambino, Mini Rev. Med. Chem. 4 (2004) 31–39.
- [4] S.N.J. Moreno, R.P. Mason, R. Docampo, J. Biol. Chem. 259 (1984) 6298–6305.
- [5] S.N.J. Moreno, R. Docampo, R.P. Mason, W. Leon, A.O.M. Stoppani, Arch. Biochem. Biophys. 218 (1982) 585–591.
- [6] R. Docampo, S.N.J. Moreno, A.O.M. Stoppani, W. Leon, F.S. Cruz, F. Villalta, R. F. Muniz, Biochem. Pharmacol. 30 (1981) 1947–1951.
- [7] A. Perez-Rebolledo, L.R. Teixeira, A.A. Batista, A.S. Mangrich, G. Aguirre, H. Cerecetto, M. González, Paola Hernández, A.M. Ferreira, N.L. Speziali, H. Beraldo, Eur. J. Med. Chem. 43 (2008) 939–948.
- [8] R.A. Sanchez-Delgado, A. Amzelotti, Mini Rev. Med. Chem. 4 (2004) 23–30.
- [9] L. Otero, G. Aguirre, L. Boiani, A. Denicola, C. Rigol, C. Olea-Azar, J.D. Maya, A. Morello, M. González, D. Gambino, H. Cerecetto, Eur. J. Med. Chem. 41 (2006) 1231–1239.
- [10] H. Cerecetto, M. González, Mini Rev. Med. Chem. 8 (2008) 1355–1383.
- [11] C. Rodrigues, A.A. Batista, R.Q. Aucélio, L.R. Teixeira, L. do Canto Visentin, H. Beraldo, Polyhedron 27 (2008) 3061–3066.
- [12] P. Sengupta, R. Dinda, S. Ghosh, W. Sheldrick, Polyhedron 22 (2003) 447–453.
- [13] A.A. Batista, M.O. Santiago, C.L. Donnici, I.S. Moreira, P.C. Healy, S.J. Berners-Price, S.L. Queiroz, Polyhedron 20 (2001) 2123–2128.
- [14] S. Bollo, L.J. Nunez-Vergara, M. Bonta, G. Chauviere, J. Perie, J.A. Squella, J. Electroanal. Chem. 511 (2001) 46–54.
- [15] J.C.M. Cavalcanti, N.V. Oliveira, M.A.B.F. de Moura, R. Fruttero, M. Bertinaria, M. O.F. Goulart, J. Electroanal. Chem. 571 (2004) 177–182.
- [16] P.C. Mandal, J. Electroanal. Chem. 570 (2004) 55–61.
- [17] S. Bollo, L.J. Nunez-Vergara, J.A. Squella, J. Electroanal. Chem. 562 (2004) 9–14.
- [18] A. Perez-Rebolledo, O.E. Piro, E.E. Castellano, L.R. Teixeira, A.A. Batista, H. Beraldo, J. Mol. Struct. 794 (2006) 18–23.
- [19] L.J. Farrugia, J. Appl. Crystallogr. 30 (1997) 565–565.
- [20] M. Navarro, T. Lehmann, E.J. Cisneros-Fajardo, A. Fuentes, R.A. Sánchez-Delgado, P. Silva, J.A. Urbina, Polyhedron 19 (2000) 2319–2325.
- [21] E. Holler, W. Schaller, B. Keppler, Arzneim. Forsch 41 (1991) 1065.
- [22] F. Kratz, M. Hartmann, B. Keppler, L. Messori, J. Biol. Chem. 269 (1994) 2581–2588.

- [23] Enraf-Nonius, COLLECT. Nonius BV, Delft, The Netherlands, 1997–2000.
- [24] Z. Otwinowski, W. Minor, in: C.W. Carter Jr., R.M. Sweet (Eds.), *Methods in Enzymology*, vol. 276, Academic Press, New York, 1997, pp. 307–326.
- [25] P. Coppens, L. Leiserowitz, D. Rabinovich, *Acta Crystallogr.* 18 (1965) 1035G.
- [26] (a) M. Sheldrick, SHELXS-97. Program for Crystal Structure Resolution. University of Gottingen, Gottingen, Germany, 1997;
(b) M. Sheldrick, SHELXL-97. Program for Crystal Structures Analysis. University of Gottingen, Gottingen, Germany, 1997.
- [27] L.J. Farrugia, *J. Appl. Crystallogr.* 32 (1999) 837–838.
- [28] S.L. Queiroz, A.A. Batista, G. Oliva, M.T. Gambardella, R.H.A. Santos, K. S. MacFarlane, S.J. Rettig, B.R. James, *Inorg. Chim. Acta* 267 (1998) 209–221.
- [29] L. Fernandez, M. Calderón, M. Martinelli, M. Strumia, H. Cerecetto, M. González, J.J. Silber, M. Santo, *J. Phys. Org. Chem.* 21 (2008) 1079–1085.
- [30] R. Hinojosa Valdez, L.T. Düsman Tonin, T. Ueda-Nakamura, B.P. Dias Filho, J. A. Morgado-Diaz, M. Sarragiotto, C. Vataru Nakamura, *Acta Trop.* 110 (2009) 7–14.